Nat Hazards (2014) 73:829–847
DOI 10.1007/s11069-014-1110-y

ORIGINAL PAPER

Two types of multiple solutions for microseismic source location based on arrival-time-difference approach

Nan Li · Maochen Ge · Enyuan Wang

Received: 5 January 2014 / Accepted: 24 February 2014 / Published online: 6 March 2014

Abstract The arrival-time-difference approach is the dominant source location approach used in the microseismic source location area. Multiple solutions problem is one of the major concerns in microseismic source location, which is closely related to the microseismic network. This paper categorizes the multiple solutions into two types based on the origin times when using the arrival-time-difference approach. Type I multiple solutions are those which have the same origin time; type II multiple solutions are those with different origin times. The sufficient and necessary conditions to produce type I multiple solutions are that all sensors are located in a straight line for two-dimensional cases and on a plane for three-dimensional cases. The sufficient and necessary conditions to produce type II multiple solutions are that all sensors are located on a hyperbola for two-dimensional cases and on a hyperboloid for three-dimensional cases. Furthermore, the proofs indicate that type I multiple solutions are preventable, while a microseismic network consisting of the minimum number of sensors can never be free of type II multiple solutions. It means, besides the minimum number of sensors, at least one more sensor which is not on this hyperbola or hyperboloid is needed to uniquely determine a source. The results from field tests and applications indicate that when the sensors of a network lie on a hyperbola, the type II multiple solutions may not be the necessary outcome under the influence of errors in

N. Li · E. Wang
State Key Laboratory of Coal Resources and Safe Mining, China University of Mining and Technology, Xuzhou 221116, Jiangsu, China

N. Li (✉) · E. Wang
School of Safety Engineering, China University of Mining and Technology, Xuzhou 221116, Jiangsu, China
e-mail: nanlitop@gmail.com

N. Li · E. Wang
Key Laboratory of Gas and Fire Control for Coal Mines, China University of Mining and Technology, Xuzhou 221008, Jiangsu, China

M. Ge
Mining Engineering Department, Missouri University of Science and Technology, Rolla, MO 65409, USA

real data. However, the accuracy of the microseismic source location is affected significantly by this kind of networks. The results also show that not only the multiple solutions problem can be avoided effectively, but more importantly, the accuracy of the source location will be greatly improved by the optimization of network based on the characteristics of the microseismic network and field conditions.

Keywords Microseismic source location · Arrival-time-difference approach · Multiple solutions · Microseismic network · Origin time · Field tests and applications

1 Introduction

The microseismic technique is a real-time monitoring technique which utilizes signals generated by materials when they are stressed or deformed to study the fracture processes (Hardy 2003; Ge 2005). It was first utilized to study the rockbursts in deep hard rock mines (Obert and Duvall 1942; Cook 1964; Obert 1975). At present, this technique is in use, or under evaluation, for stability monitoring of underground structures such as mines, tunnels, and geothermal engineering, as well as surface structures such as foundations, rock and soil slopes, and dams (Baria and Batchelor 1985; Luo and Hatherly 1998; Hardy 2003; Ge 2005; Jiang et al. 2006; Hirata et al. 2007; Li 2009; Xu et al. 2011). In theoretical and practical perspectives, source location is one of the most classical and basic objectives and the most valuable feature of the microseismic technique due to its ability to delineate the unstable areas (Tian and Chen 2002; Ge 2005; Gong et al. 2010).

An accurate and stable source location solution depends on many factors. A suitable source location method and a microseismic network are two key factors contributing to microseismic source location accuracy (Hardy 2003; Gong et al. 2010). Most of the source location methods in microseismic studies are based on the arrival-time-difference approach (Ge 2003a, b), such as the USBM method (Leighton and Blake 1970; Leighton and Duvall 1972), the Geiger's method (Geiger 1910, 1912), the Inglada's method (Inglada 1928), the Thurber method (Thurber 1985), the Powell method (Tang 1979), the genetic algorithm (Sambridge and Gallagher 1993; Gong et al. 2012), the simplex method (Prugger and Gendzwill 1988), the particle swarm method (Chen et al. 2009; Shishay et al. 2012), and some other methods (Dong et al. 2011; Zhu et al. 2013). Mathematically, the essence of the arrival-time-difference approach is to establish and solve a set of nonlinear equations which include the coordinates and the origin time of the source. Theoretical research and practical applications show that there may exist multiple solutions when the microseismic network layout is not good enough (Ge and Hardy 1988; Gong et al. 2010). Generally, this problem can be solved based on the consideration of the physical restraints in some cases. But in other cases, there may exist more than one source satisfying all the physical restraints. Therefore, a thorough probe of the multiple solutions problem associated with the geometrical characteristics of the microseismic network should be studied.

In general, the research regarding the multiple solutions problem in microseismic source location has been limited. As early as the beginning of the twentieth century, Inglada (1928) observed the phenomenon of multiple solutions in source location process. He found that multiple solutions could be avoided to certain extent by changing the coordinates of the sensors. Cete (1977) also noticed that the Inglada's method had multiple solutions which were sometimes all physically feasible. Gong et al. (2012) found that some microseismic network layouts may cause multiple solutions, while others can yield the only true source when he studied the optimal configuration of seismological observation network. Kijko and Sciocatt's research showed that the spatial distribution of seismic stations played a significant role in the seismic network performance, but their study did not involve the relationship between the multiple solutions and seismic network (Kijko 1977a, b; Kijko and Sciocatt 1995).

Rindorf is another person who has been deeply involved in the study of the multiple solutions and the effect of network configuration. His major contribution is the proof that there are at most two physically feasible solutions for source location methods based on the arrival-time-difference approach (Rindorf 1981, 1984). Xu et al. (2008) studied the impact of sensor deployment on the uniqueness of source estimation in Euclidean plane and inside a simple polygon. They derived the minimum number of sensors needed for uniquely identifying a source for each case. They also present some other important results: The arrival-time-difference localization uniquely identifies a source in Euclidean plane only when the sensors do not lie on a hyperbola, and two hyperbolas that correspond to arrival-time-difference to a source have at most 2 intersections. However, they did not classify the multiple solutions for further study. Actually, they merely studied one type of multiple solutions (when non-collinear sensors are used, namely type II multiple solutions in the following study), but did not consider the other type of multiple solutions (when all sensors are collinear, namely type I multiple solutions in the following study). In addition, their research did not refer to three-dimensional cases.

To address the above problems, we first divide the multiple solutions into two types based on the physical meaning of the source parameter. And then, we demonstrate the sufficient and necessary conditions for two types of multiple solutions not only in two-dimensional plane but also in three-dimensional space. Next, we discuss the multiple solutions problem for seismic networks with the minimum number of sensors and with more than the minimum number of sensors. In the end, the field test and applications related to multiple solutions and microseismic network are carried out to demonstrate the practical importance of this study.

2 Arrival-time-difference approach and classification of multiple solutions

2.1 Source location equation and hyperbola (hyperboloid)

There are two main types of waves, namely P wave and S wave, generated by the microseismic events. In general, the velocity of P wave is much higher than S wave. For coal and rock materials, the velocity for S waves is typically 60 % of that for P waves (Hardy 2003). Compared with earthquake, the regions monitored by the microseismic technique are relatively small, and the microseismic signals are often associated with considerable background noise. The first arrival time of S wave is often buried by coda wave of P wave and cannot be determined. Therefore, the first arrival time of P wave is widely used in microseismic source location.

In practice, the P wave velocities for microseismic source location are measured by blasting tests in site. And then, the mean of the measured velocities applies to all stations. As shown in Fig. 1, the arrival-time-difference approach is initially described by a set of nonlinear equations which has the form (Hardy 2003; Gibowicz and Kijko 1994):

$$\sqrt{(x_i - x_0)^2 + (y_i - y_0)^2 + (z_i - z_0)^2} = v\,(t_i - t_0) \tag{1}$$

where t_0 is the origin time of the source; t_i is the arrival time at the ith sensor; v is the P wave velocity. $i = 1,2\ldots m$, and here, m denotes the number of equations and it equals the number of receivers.

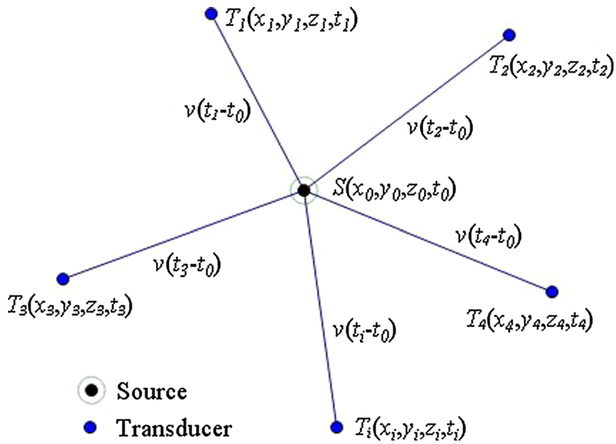

Fig. 1 Schematic of source location based on the arrival-time-difference approach

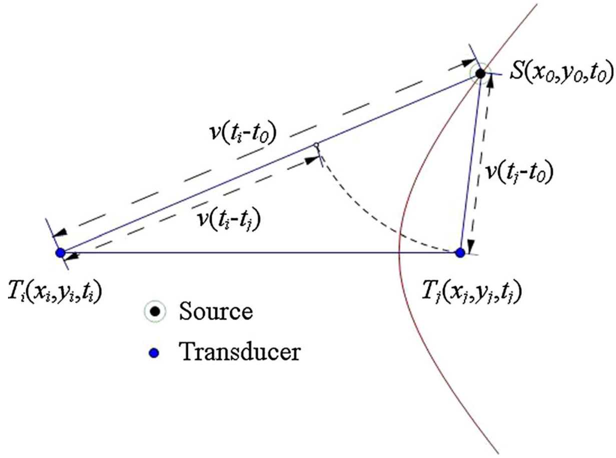

Fig. 2 A hyperbola determined by the arrival-time-difference approach at two sensors in a plane

Equation (1) is rearranged in the following to extract some crucial information needed for this study. Subtracting the jth from the ith equation leads to (Ge and Hardy 1988):

$$R_i - R_j = v(t_i - t_j) \tag{2}$$

Here, R_i is Euclidean distance between the ith sensor and the source, $R_i = \sqrt{(x_i - x_0)^2 + (y_i - y_0)^2 + (z_i - z_0)^2}$.

Geometrically, Eq. (2) means that the source track determined by two sensors is a hyperboloid in three-dimensional space and a hyperbola in two-dimensional space (for convenience, the terms hyperbola and hyperboloid are used to refer to a portion of a hyperbola and hyperboloid in this paper). Figure 2 shows a hyperbola in a plane. The difference in distances of any point on a hyperbola or hyperboloid from its foci is a constant, which equals $v(t_i - t_j)$ in the case of source location analysis (Fig. 2). In this regard, the essence of source location based on the arrival-time-difference approach is to find the common intersection of a set of hyperboloids or hyperbolas.

2.2 Classification of multiple solutions

For a set of nonlinear equations, the solutions are usually multiple. Theoretically, there are 2^4 solutions if Eq. (1) is squared on both sides. However, among these 16 possible solutions, there will be many, which may not be physically feasible. The term "physically feasible" here means that the solutions must be in the real domain and must satisfy the physical restraints.

For the convenience of later analysis, multiple solutions in this study are categorized into two types, type I and type II. Type I multiple solutions are those that have the same origin time; type II multiple solutions are those with different origin times. The reason for this classification will be analyzed in the main body of this paper.

3 Multiple solutions with the same origin time

3.1 Proofs of necessary and sufficient conditions of type I multiple solutions

3.1.1 Necessary condition of type I multiple solutions

Let $T_i(x_i, y_i)$, $i = 1, 2, 3,\ldots m$, be sensors in a plane. The arrival times from the source to these sensors are t_i, and the velocity is v. As shown in Fig. 3, draw a circle with the center at T_1 and with the radius vt_1. Similarly, draw a circle for T_2. These two circles intersect at S_1 and S_2. Using S_1 and S_2 as the centers, draw two circles with the radius vt_3. These two circles intersect at B_1 and B_2, and either B_1 or B_2 can be chosen as the position of T_i. S_1 and S_2 are the common solutions with the same origin time for all sensors due to the fact that S_1 and S_2 are equally distant from each sensor. Therefore, type I multiple solutions consist of two solutions.

Based on geometry theorems, it can be proved that line S_1S_2 is perpendicular to and bisected by line T_1T_2 and B_1B_2. Therefore, T_1T_2 and B_1B_2 coincide. So, for a two-dimensional source location, the necessary condition to produce type I multiple solutions is that all sensors have to be in a straight line.

3.1.2 Sufficient condition of type I multiple solutions

Let sensors, T_1, T_2, and T_i, be on a straight line as shown in Fig. 4. The arrival times at these sensors are t_1, t_2, and t_i, respectively. The source is somewhere off this straight line.

According to Eq. (2), a hyperbola that passes through the source can be determined for each pair of the sensors based on the arrival times received at these sensors. Two such hyperbolas based on the information from sensors T_1 and T_i, and T_2 and T_i are shown in Fig. 4. These two hyperbolas are symmetrical about the same line when sensors are on a straight line. Hence, these hyperbolas intersect not only at the source, but also at another point, the mirror image of the source relative to the straight line. In Fig. 4, these two points are marked as S_1 and S_2, and the travel times from these two points to each sensor are the same. So, the origin times for both possible sources are the same.

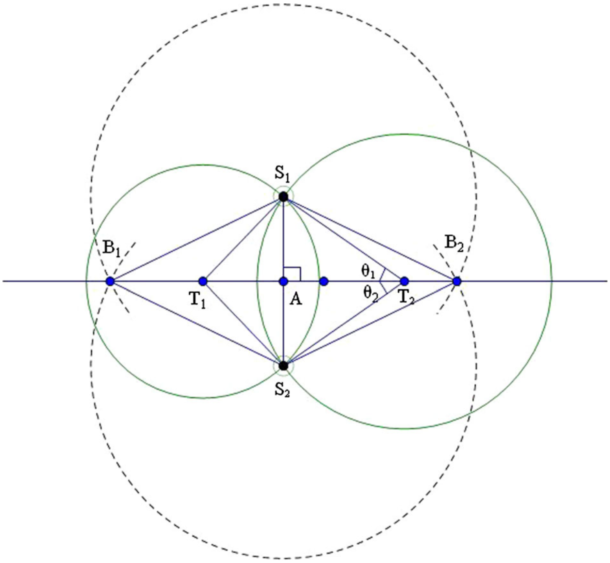

Fig. 3 Geometrical meaning of the necessary condition for type I multiple solutions

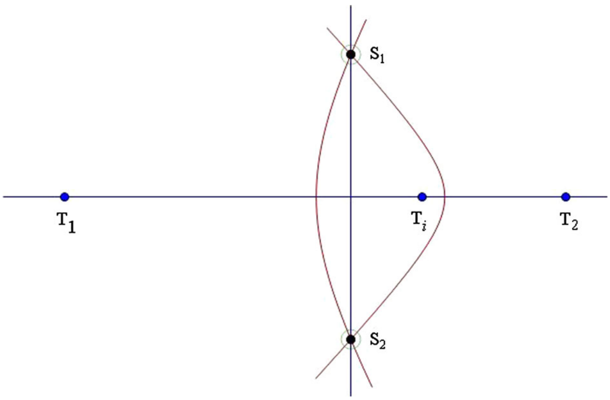

Fig. 4 Geometrical meaning of the sufficient condition for type I multiple solutions

Based on the above proof, the sufficient condition for two-dimensional source location can be stated as follows: Type I multiple solutions are always the case as long as all sensors remain on a straight line.

3.2 Results

From the previous proofs, the sufficient and necessary conditions to produce type I multiple solutions for two-dimensional cases are that such solutions occur if and only if all sensors are located on a straight line. From these proofs, it can also be concluded that type I multiple solutions consist of two solutions and they are symmetrical about the straight line passing through all sensors.

In principle, all the conclusions made for two-dimensional cases can be generalized to three-dimensional cases. Since the proof procedures are almost identical, only the conclusions will be presented here.

Type I multiple solutions are always the result if and only if all sensors are in a plane. Specifically speaking, according to the spatial position of sensors, type I multiple solutions can be subdivided into the following two situations: First, when all sensors are in a plane and not in a straight line, multiple solutions consist of two solutions and they are symmetrical about this plane passing through these sensors (Fig. 5a). Second, when all sensors are on a straight line, the number of solutions is infinite and they form a circle which is perpendicular to the straight line with the center on it (Fig. 5b).

Based on these conclusions, it is clear that in order to prevent type I multiple solutions, the network layout should not be on a straight line for two-dimensional problems and should not be on a plane for three-dimensional problems.

4 Multiple solutions with different origin times

4.1 Proofs of necessary and sufficient condition of type II multiple solutions

From Rindorf's proof, it is known that type II multiple solutions problem consists of two solutions (Rindorf 1981, 1984). Xu et al. (2008) studied properties of sensor sets that uniquely identify all sources in Euclidean space. They found that the arrival-time-difference approach can uniquely identify a source in plane only if all sensors do not lie on a hyperbola. But their research did not refer to three-dimensional cases. A totally different method is presented to prove the necessary and sufficient conditions of type II multiple solutions. Through this new method, the conclusions can be generalized to three-dimensional cases.

4.1.1 Necessary condition of type II multiple solutions

As illustrated in Fig. 6, suppose $T_i(x_i, y_i)$, $i = 1, 2, 3, \ldots m$, is the ith sensor in a plane. Suppose $S_1(x_{01}, y_{01}, t_{01})$ and $S_2(x_{02}, y_{02}, t_{02})$ are the multiple solutions with different origin times determined by this network layout.

Based on Eq. (2) and the initial conditions, for sources, S_1 and S_2, the following equations can be constructed:

$$\sqrt{(x_i - x_{01})^2 + (y_i - y_{01})^2} = v(t_{i1} - t_{01}) \tag{3}$$

$$\sqrt{(x_i - x_{02})^2 + (y_i - y_{02})^2} = v(t_{i2} - t_{02}) \tag{4}$$

where t_{i1} and t_{i2} are the arrival times at the ith sensor from sources S_1 and S_2, respectively.

Since both S_1 and S_2 are the solutions, the arrival time, at each sensor of this network layout from S_1 and S_2, must be the same, namely $t_{i1} = t_{i2}$. Subtracting Eq. (4) from Eq. (3), it yields

$$\left|\sqrt{(x_i - x_{01})^2 + (y_i - y_{01})^2} - \sqrt{(x_i - x_{02})^2 + (y_i - y_{02})^2}\right| = |v(t_{02} - t_{01})| \tag{5}$$

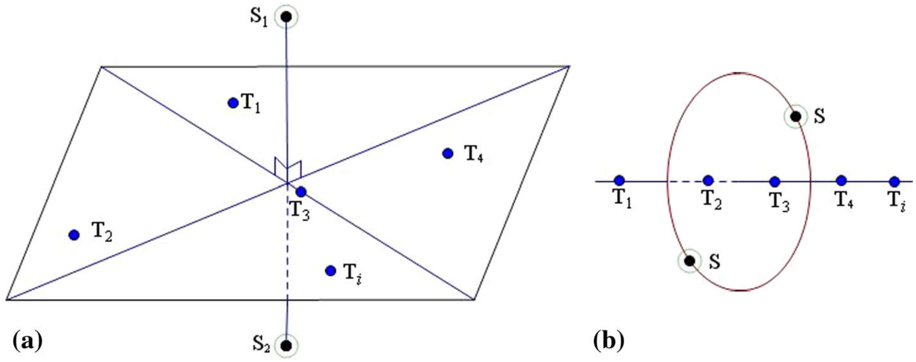

Fig. 5 Source distribution of type I multiple solution in the three-dimensional space

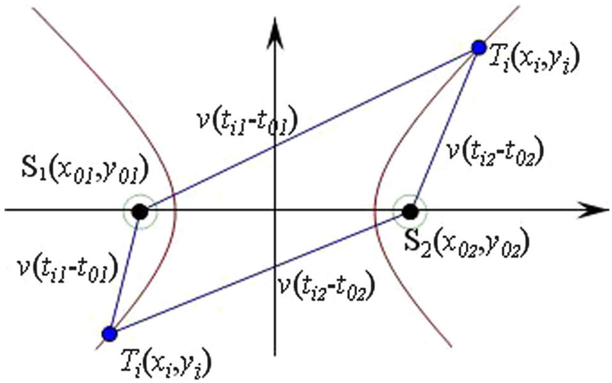

Fig. 6 Geometrical meaning of the necessary condition for type II multiple solutions

Equation (5) shows that the trace of the ith sensor is a hyperbola with the foci at S_1 and S_2. The distance difference in any position of this sensor from the foci is equal to $|v(t_{02} - t_{01})|$.

From the above analysis, the necessary condition for a network layout to have type II multiple solutions for two-dimensional cases can be stated as follows: If there are type II multiple solutions, then the sensors in the associated network must be located on a hyperbola.

4.1.2 Sufficient condition of type II multiple solutions

Let all the sensors, $T_i(x_i, y_i)$, $i = 1, 2, 3, \ldots m$, be on a hyperbola which has the foci at $S_1(x_{01}, y_{01})$ and $S_2(x_{02}, y_{02})$. The distance difference in any point on this hyperbola from S_1 and S_2 is equal to d. The velocity is v. As shown in Fig. 7, for convenience, assume $|T_iS_1| > |T_iS_2|$. Consider S_1 as one source and assume its origin time as t_{01}. Consider S_2 as another source. Let the origin time for t_{02} be

$$t_{02} = t_{01} + \frac{d}{v} \tag{6}$$

As illustrated in Fig. 7, the following equations can be constructed:

$$|T_iS_1| = v(t_{i1} - t_{01}) \tag{7}$$

$$|T_iS_2| = v(t_{i2} - t_{02}) \tag{8}$$

where t_{i1} and t_{i2} are the arrival times at the ith sensor from sources S_1 and S_2, respectively. Solving the above equations, the following equation is derived:

$$t_{i1} = t_{i2} \tag{9}$$

Then, both S_1 and S_2 will give the same arrival time information for each point on this hyperbola. In other words, S_1 and S_2 are the two sources for this microseismic network. Therefore, the sufficient condition for a microseismic network to have type II multiple solutions in two-dimensional cases is that all sensors are located on a hyperbola.

4.1.3 Results

Based on the above proofs, the necessary and sufficient condition of type II multiple solutions for three-dimensional cases can be directly obtained. Since the proof procedures are almost identical, only the conclusions will be presented here. The sufficient and necessary conditions for microseismic network to have type II multiple solutions are if and only if all the sensors are on a hyperbola in plane or on a hyperboloid in space. In addition, the proofs show that the two solutions are located at the foci of the hyperbola or the hyperboloid.

Besides, the results reveal that type II multiple solutions are a phenomenon closely related to the geometry of seismic network. These proofs show that type II multiple solutions are not the necessary outcome of the arrival-time-difference approach, and seismic network can be entirely free of type II multiple solutions as long as all the sensors are not on a hyperbola or hyperboloid.

Based on the above analysis, it is immediately understood that the geometric conditions for a microseismic network layout to produce type II multiple solutions are different from the conditions to produce type I multiple solutions. This is why multiple solutions are categorized into two groups.

4.2 The seismic network with the minimum number of sensors

The Inglada's method only requires the minimum number of sensors (three sensors for the two-dimensional cases and four sensors for the three-dimensional cases) to locate the microseismic sources. Cete (1977) and Rindorf (1981, 1984) studied type II multiple solutions using Inglada's method. They found that for a microseismic network consisting of the minimum number of sensors, there were always type II multiple solutions which commonly occur in certain areas. Xu et al. (2008) found that three sensors are not sufficient for unique localization of a source in Euclidean plane. But they did not get involved in the three-dimensional cases for the network with the minimum number of sensors. We first demonstrate that a microseismic network consisting of the minimum number of sensors can never be free of type II multiple solutions in two-dimensional plane. Based on the two-dimensional proof, we have further proved that four sensors are not sufficient for uniquely determining a source in three-dimensional space.

4.2.1 Proof for two-dimensional cases with the minimum number of sensors

As shown in Fig. 8, given three points, $A(x_1, y_1)$, $B(x_2, y_2)$, and $C(x_3, y_3)$, are not on a straight line. Choose any two of these three points, such as B and C, and join them. Draw

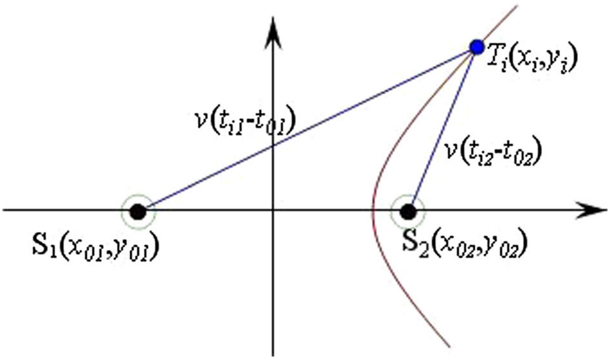

Fig. 7 Geometrical meaning of the sufficient condition for type II multiple solution

line *EF* which is perpendicular to line *BC* and bisects it. *D* is the intersection point of line *BC* and line *EF*. Join *A* and a point, such as *B*, which is on the same side of the straight line *EF* (*B* can be on line *EF*). Line *AB* should not be parallel with *EF*. This can be always achieved by carefully choosing the two initial points. (If $AB//EF$, *A* should become *A*' as shown in Fig. 8. In this case, choose *A*' and *C* as the two initial points. The following proof is similar.)

Mark the middle point of line *AB* as *G,* and from this point, draw line *GH*, which is parallel with *EF*. Draw another line *GI* from *G*, and make *GH* and *GI* be symmetrical to *AB*. Use *GH* and *GI* as the limit of asymptotes. Any hyperbola, if its asymptotes are confined by these two lines, will have two intersections with line *EF*.

Based on the fundamental properties of hyperbolas, the hyperbola defined by the following equation is confined between *GH* and *GI*.

$$\sqrt{(x-x_2)^2+(y-y_2)^2}-\sqrt{(x-x_1)^2+(y-y_1)^2}=2a, \quad \text{and} \quad \text{satisfy} a<c \tag{10}$$

where (x_1, y_1) and (x_2, y_2) are the coordinates of *A* and *B* which are also the foci of the hyperbola defined by Eq. (10). The difference in distances of any point on this hyperbola from its foci is $2a$. The distance between *A* and *G* is *c*.

As discussed above, a hyperbola, such as hyperbola I (Fig. 8), defined by Eq. (10) has two intersections with line *EF*. Assuming the coordinates of these two intersections be $S_1(x_{01}, y_{01})$ and $S_2(x_{02}, y_{02})$.

Substitute $S_1(x_{01}, y_{01})$ and $S_2(x_{02}, y_{02})$ into Eq. (10), respectively,

$$\sqrt{(x_{02}-x_2)^2+(y_{02}-y_2)^2}-\sqrt{(x_{02}-x_1)^2+(y_{02}-y_1)^2}=2a \tag{11}$$

$$\sqrt{(x_{01}-x_2)^2+(y_{01}-y_2)^2}-\sqrt{(x_{01}-x_1)^2+(y_{01}-y_1)^2}=2a \tag{12}$$

Subtract Eq. (12) from Eq. (11) and rearrange the resulting equation, the following equation is derived:

$$\begin{aligned}&\sqrt{(x_2-x_{02})^2+(y_2-y_{02})^2}-\sqrt{(x_2-x_{01})^2+(y_2-y_{01})^2}\\&=\sqrt{(x_1-x_{01})^2+(y_1-y_{01})^2}-\sqrt{(x_{01}-x_{02})^2+(y_1-y_{02})^2}\end{aligned} \tag{13}$$

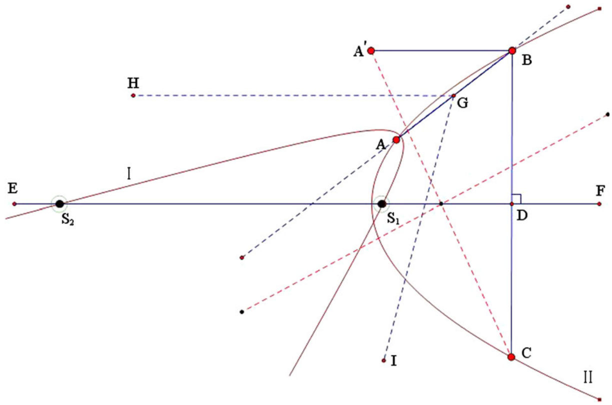

Fig. 8 A hyperbola passes through three non-collinear points in a plane

It is indicated from Eq. (13) that the difference in distances of A from S_2 and S_1 is the same as that of B. Since A, B, S_1, and S_2 are known points, this difference is a constant and we denote it as d. Since line BC is perpendicular to and bisected by line EF, the difference in distances of C from S_2 and S_1 is equal to d as well. So, there must be a hyperbola II with the foci at S_1 and S_2 which passes through A, B, and C. The equation of hyperbola II is as follows:

$$\sqrt{(x-x_{02})^2+(y-y_{02})^2}-\sqrt{(x-x_{01})^2+(y-y_{01})^2}=d,\quad \text{and} \quad \text{satisfy} d<e \tag{14}$$

where e is the distance from S_1 to S_2.

As can be seen from the above analysis, a used in Eq. (10) and d used in Eq. (14) can be arbitrarily as long as $a < c$ and $d < e$. Therefore, there are an infinite number of hyperbolas which can pass through three sensors in a plane.

4.2.2 Proof for three-dimensional cases with the minimum number of sensors

As shown in Fig. 9, there are any four points, $A(x_1, y_1, z_1)$, $B(x_2, y_2, z_2)$, $C(x_3, y_3, z_3)$, and $D(x_4, y_4, z_4)$, in a three-dimensional space. These four points are not coplanar. Since these four points are in a three-dimensional space, it implies that no three points are on a straight line; otherwise, these four points will be in a two-dimensional space. Therefore, there must be a circle which passes through any three points.

Draw a circle which connects any three points, say, A, B, and C. Mark the center of this circle as G. Draw a straight line OF which is perpendicular to this circle and passes through the center G. Draw a plane, h, which contains line OF and point D. Plane h will intersect the circle at M and N.

Since D, M, and N are three non-collinear points on plane h, there is at least one hyperbola which, as proved earlier, passes through these three points and is also symmetrical about line OF (Fig. 9).

Use line OF as the axis to rotate this hyperbola to form a hyperboloid. The circle with A, B, C, M, and N on it is on this hyperboloid. Since D is on this hyperbola, D is also on this hyperboloid. So, A, B, C, and D are all on this hyperboloid. This also proves that there must

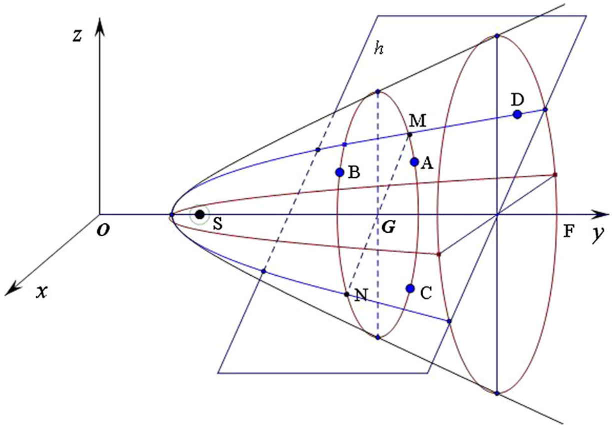

Fig. 9 A hyperboloid passes through four points which are not coplanar in the three-dimensional space

exist a hyperboloid that passes through any four non-coplanar points in a three-dimensional space.

These proofs show that one can always find a hyperbola or hyperboloid passing through the minimum number of sensors in two-dimensional plane and three-dimensional space. The proof procedures also demonstrate that there are an infinite number of hyperbolas or hyperboloids which can pass through these sensors. In addition, these proofs explain why Cete (1977) sometimes got multiple solutions when he used the Inglada's method as well.

4.3 The microseismic network with more than the minimum number of sensors

When a microseismic network consists of more than the minimum number of sensors, it is very unlikely that all sensors will be completely on a hyperbola or a hyperboloid. Xu et al. (2008) have proved that four sensors at the corners of a parallelogram can uniquely identify a source in Euclidean plane. Here, the other two typical four-sensor networks as shown in Fig. 10 will be analyzed. Through this analysis, it will be demonstrated that, besides the minimum number of sensors, at least one more sensor is needed to determine the true source.

The major characteristic of the first type of network shown in Fig. 10 is that three sensors are on a straight line. Since there are at most two intersections, when a straight line intersects a hyperbola, all sensors in this type of array cannot be on a hyperbola.

For the second type of network, we first connect four points sequentially to form a closed loop. As shown in Fig. 11b, the way of connecting these points can be arbitrary and the curve between any two points need not be straight as long as the region inside the loop is simply connected. Draw a straight line with the following characteristics: (1) parallel to one of the sides of the triangle and this side must be the one defined by two sensors that have been directly connected with the inner sensor and (2) between this side and the sensor inside the triangular area. Line EE' shown in Fig. 11c is a such straight line.

Ignoring anyone of these curves, line EE' still intersects with three curves, and in other words, there are at least three intersections. And then, straight line EE' would have three intersections with this hyperbola if these sensors were on a hyperbola. However, this has been shown to be impossible. So the second type of array is not on a hyperbola.

Fig. 10 Two typical types of four-sensor networks

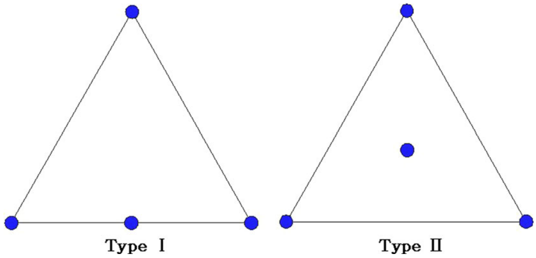

Fig. 11 Geometrical analysis of the second type of network

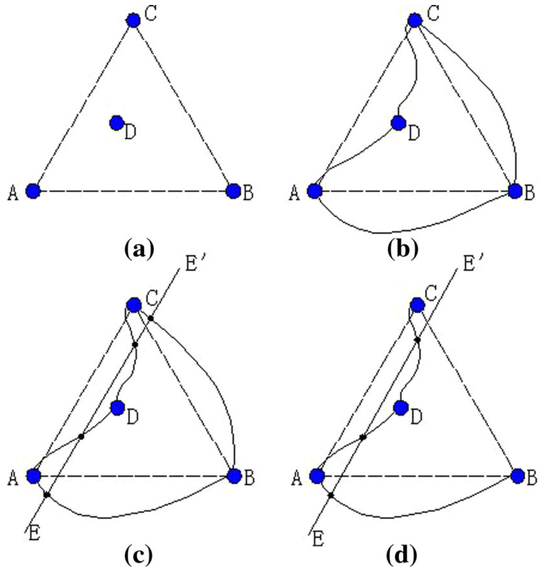

5 Field tests and applications

Qianqiu Coal Mine is located in Yima, Henan Province, China. It is a deep coal mine with an average mining depth of 830 m. At present, the main mining seam is 2–1 coal with the average inclination 10°, the working faces 141 and 172 are doing mining operations, the working face 192 is in shutdown state, and 112 is an excavation working face. Rockbursts and coal bumps are the main threat to this mine safety. In Qianqiu Coal Mine, a total of 33 rockbursts were reported in the last 5 years. The ARAMIS M/E microseismic monitoring system with 16 channels (a product of The Institute of Innovative Techniques (EMAG) at Katowice, Poland) was installed to monitor the microseismic activities and study the rockbursts and coal bumps. At present, 14 microseismic sensors are employed. As shown in Fig. 12, they are installed in the roadways of working faces 141, 112, 172, 192, and track roadways.

Based on the theory of the mining pressure and ground control, the balance of in situ stress will be broken and form a new balance of the mining-induced stress due to the mining activities (Qian and Shi 2003; Cao and Dou 2008). The distribution of the mining-induced stress in front of the working face is illustrated in Fig. 13. According to the measured data of the mining-induced stress in Qianqiu Coal Mine, the advanced

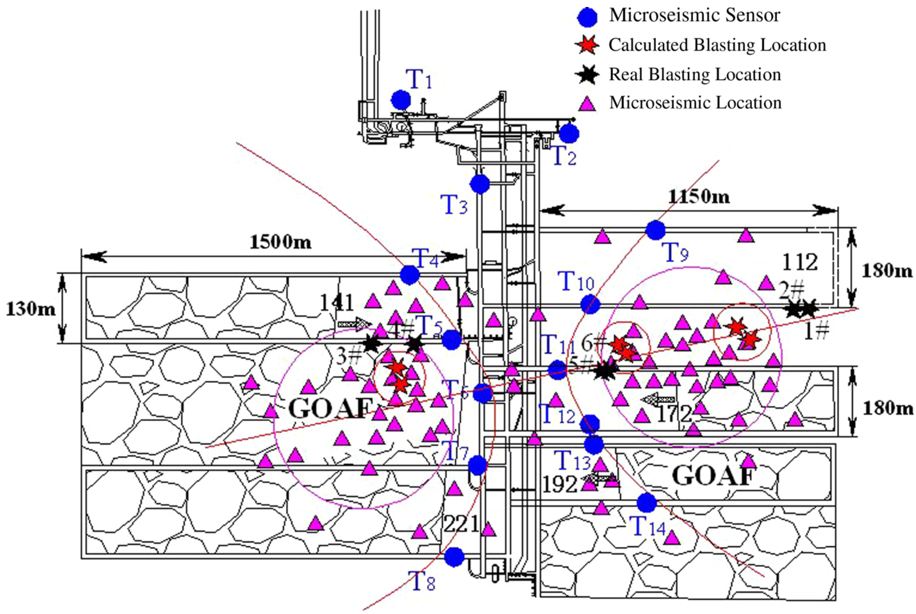

Fig. 12 The microseismic network layout and the microseismic source location before the optimization of network

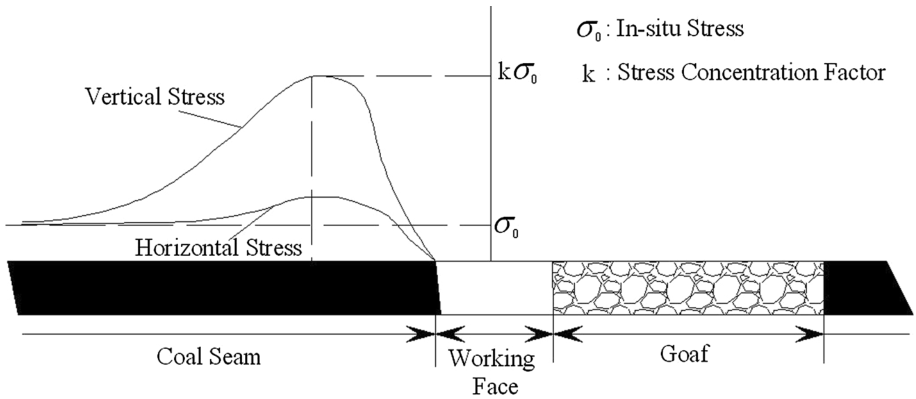

Fig. 13 Schematic of mining-induced distribution on the mining side coal seam

influencing areas of the mining-induced stress are 100–200 and 30–80 m in working faces and excavation working faces, respectively (Xia et al. 2011).

Figure 12 shows the microseismic event locations resulting from the original microseismic network in December 2012. It is clearly shown that most microseismic events are located at the goaf zone between the working faces 141 and 221, and the goaf zone behind the working face 172. Obviously, they are not realistic locations in this longwall mining environment. In addition, type II multiple solutions often happened during location processes. Meanwhile, the blasting test was carried out to further check the performance of the

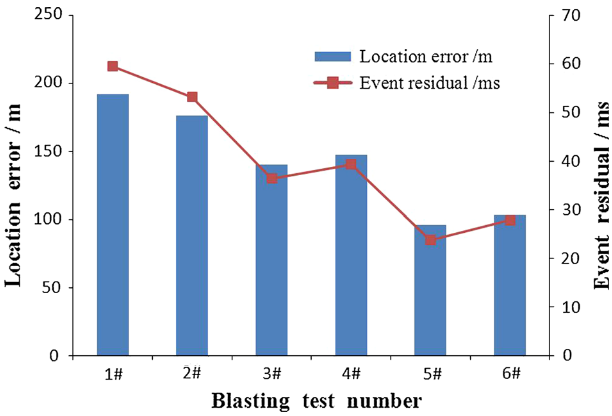

Fig. 14 Source location errors and event residuals for six blasting tests before the optimization of network

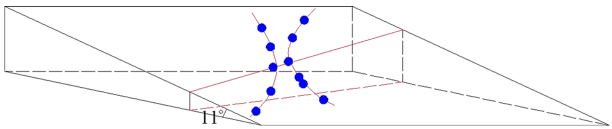

Fig. 15 Two hyperbolas pass through the rest sensors

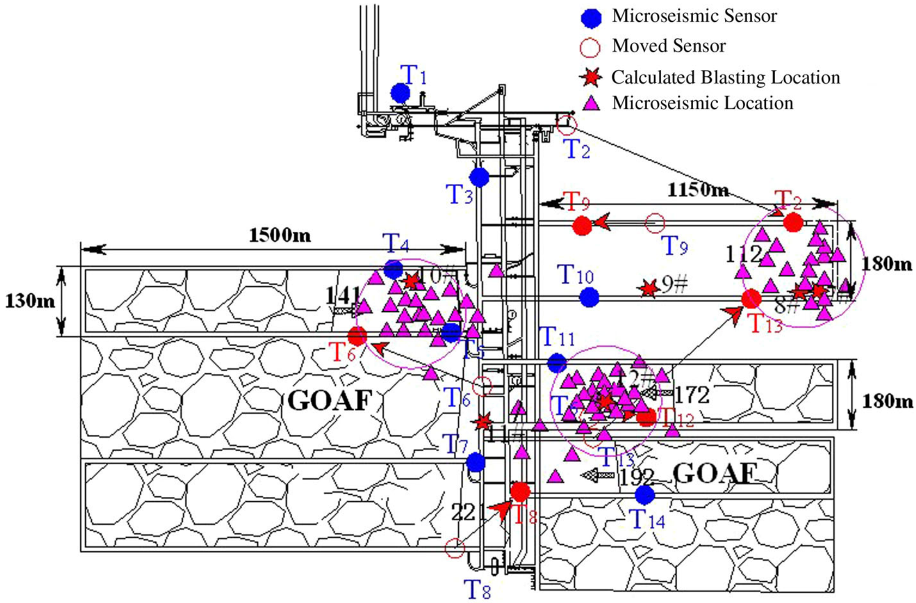

Fig. 16 The microseismic network layout and the microseismic source location after the optimization of network

Table 1 Source location results for blasting tests after the optimization of network

Blasting test number	Blasting location	Coordinates/m			Location error/ m	Event residual/ ms
		x	*y*	*z*		
7#	Real location	5,457.5	3,009.5	−8	16.5	6.1
	Calculated location	5,442.8	3,016.9	−6.6		
8#	Real location	5,486.5	2,978.5	−10	11.1	8.4
	Calculated location	5,497.2	2,976.3	−12.2		
9#	Real location	4,798.5	2,908	−52	15.2	5.5
	Calculated location	4,787.2	2,905.5	−61.9		
10#	Real location	4,209.5	2,966.5	−49	9.5	3.7
	Calculated location	4,200.6	2,963.6	−47.5		
11#	Real location	4,827	2,575	−141	18.7	7.0
	Calculated location	4,812	2,566.8	−133.4		
12#	Real location	4,490	2,512	−143	10.8	4.2
	Calculated location	4,484.8	2,506.4	−135.3		

microseismic network and the accuracy of the source location. Although the multiple solutions did not always appear, the accuracy of the source locations was really terrible. The results from Fig. 14 show that location errors reached a plateau at 150 m with very large event residuals from 23.8 to 59.5 ms.

After studying the geometrical characteristics of this microseismic network in detail, we found that sensors T1, T2, and T3 are far away from the key monitoring areas. And they cannot receive valid microseismic signals in many cases because of the complicated geological conditions and the complicated roadway layout and the goafs caused by mining activities. It is indicated from Figs. 12 and 15 that the rest microseismic sensors happened to be on two hyperbolas in the monitoring region. Based on the sufficient condition of type II multiple solutions, the above microseismic network will always produce type II multiple solutions. However, type II multiple solutions did not occur in all cases because of the errors of the P wave velocity and arrival times in real data, and the imperfect hyperbola. But the accuracy of the microseismic source location was reduced significantly by this network layout. As clearly shown in Fig. 12, the calculated microseismic and blasting locations are removed from the mining zone to the foci of these two hyperbolas.

Based on the above analysis, and considering local field conditions as well, a project was carried out to optimize the microseismic network. The sensors T2, T6, T8, T9, T12, and T13 were selected to redeploy. The optimized microseismic network is shown in Fig. 16.

Blasting tests were carried out to test and verify the feasibility and advantages of the optimized microseismic network. As shown in Table 1, the location errors and event residuals of the six blasting tests are controlled within 20 m and 10 ms, respectively, which can meet the requirements of microseismic source location. In addition, the microseismic source locations from April 6, 2013, to April 15, 2013, after optimizing the microseismic network are shown in Fig. 16.

As illustrated in Fig. 16, almost all of the microseismic events were located in the coal seam and immediate roof in front of the working faces 141 and 172, and the excavation working face 112, which are exactly the advanced influencing areas of the mining-induced stress. Furthermore, the phenomenon of multiple solutions did not appear. In summary, not only the microseismic network optimization can avoid multiple solutions problems effectively, but more importantly, the accuracy of the source location will be greatly improved by optimizing microseismic network.

6 Conclusions

The arrival-time-difference approach is the dominant source location approach used in the microseismic area. Multiple solutions problem is one of the major concerns in microseismic source location, which is closely related to the microseismic network. In this paper, multiple solutions were first categorized into two types. Type I multiple solutions are those featuring the same origin time, and type II multiple solutions are those featuring different origin times.

The sufficient and necessary conditions to produce type I multiple solutions are that all the sensors lie on a straight line for two-dimensional cases and on a plane for three-dimensional cases. The exact condition for a seismic network to have type II multiple solutions was found to be that this network is located on a hyperbola for two-dimensional cases and on a hyperboloid for three-dimensional cases. The revelation of this condition is one of the most important achievements of this current research since it is the first time that the cause of type II multiple solutions has been explained.

Based on these proofs, it is clearly concluded that type I multiple solutions are preventable. In contrast, it is found that there are infinite hyperbolas or hyperboloids passing through the minimum number of sensors. Thus, a seismic network consisting of the minimum number of sensors can never be free of type II multiple solutions. In addition, it is concluded that if a network is expected to be on a hyperbola or hyperboloid, besides the minimum number of sensors, at least one more sensor which is not on this hyperbola or hyperboloid is needed. Finally, it is worthwhile to note that the mathematical treatment used in this study was independent of the source location methods. Therefore, the conclusions presented have general application and are valid for any source location methods as long as the arrival-time-difference approach is utilized.

The field test and applications indicate that when the sensors lie on hyperbolas, type II multiple solutions may not occur in all cases because of the influence of errors in real data. However, the accuracy of the microseismic source location is affected significantly by this kind of networks. The results also show that not only the multiple solutions problem can be avoided effectively, but also the accuracy of the source location is greatly improved by the optimized microseismic network. It means that the optimization of network based on the characteristics of the microseismic network and field conditions is of primary importance for microseismic source location.

Acknowledgments This study is supported by the National Key Technology R&D Program of China (2012BAK04B07, 2012BAK09B01) and the Research and Innovation Program for Doctoral Candidate in Jiangsu Province (CXZZ12_0956). We thank Xuelong Li, Zhenyu Sun, Chao Yang, and Shijie Su, who joined the field tests and applications in Qianqiu Coal Mine. We also thank Dr. Bingxiang Huang and anonymous reviewers for their comments and suggestions to improve the manuscripts.

References

Baria RK, Batchelor AS (1985) Induced seismicity during the hydraulic stimulation of a potential hot dry rock geothermal reservoir, Proc. 4th Conference on acoustic emission/microseismic activity in geologic structures and materials, Clausthal-Zellerfeld, Germany, Trans Tech Publications pp 327–325

Cao A, Dou L (2008) Analysis of focal mechanism caused by rupture of stope roof. Chin J Rock Mech Eng 27:3833–3840

Cete A (1977) Seismic source location in the Ruhr District, Proceedings First Conference on acoustic emission/microseismic activity in geologic, Pennsylvania State University, Trans Tech Publications, Clausthal, Germany, pp 231–242

Chen B, Feng X, Li S, Yuan J, Xu S (2009) Microseismic sources location with hierarchical strategy based on particle swarm optimization. Chin J Rock Mech Eng 28:740–749

Cook NGW (1964) The application of seismic techniques to problems in rock mechanics. Int J Rock Mech Min Sci Geomech Abstr 1:169–179

Dong L, Li X, Tang L, Gong F (2011) Mathematical functions and parameters for microseismic source location without pre-measuring speed. Chin J Rock Mech Eng 30:2057–2067

Ge M (2003a) Analysis of source location algorithms: Part I. Overview and non-iterative methods. J Acoust Emiss 21:14–28

Ge M (2003b) Analysis of source location algorithms: Part II. Iterative methods. J Acoust Emiss 21:29–51

Ge M (2005) Efficient mine microseismic monitoring International. J Coal Geol 64:44–56

Ge M, Hardy R (1988) The mechanism of array geometry in the control of AE/MS source location accuracy, Proceedings 29th U.S. Symposium on rock mechanics, Minneapolis, USA, pp 597–605

Geiger L (1910) Herbsetimmung bei Erdbeben aus den Ankunfzeiten. K Gessell Wiss Goett 4:331–349

Geiger L (1912) Probability method for the determination of earthquake epicentres from the arrival time only. Bull. St. Louis. Univ. 8:60–71

Gibowicz SJ, Kijko A (1994) An introduction to mining seismology. Academic Press Inc, San Diego

Gong S, Dou L, Cao A (2010) Study on optimal configuration of seismological observation network for coal mine. Chin J Geophys 53:457–465

Gong S, Dou L, Ma X, Mou Z, Lu C (2012) Optimization algorithm of network configuration for improving location accuracy of microseism in coal mine. Chin J Rock Mech Eng 32:7–17

Hardy R (2003) Acoustic emission/microseismic activity. A.A. Balkema, Lisse

Hirata A, Kameoka Y, Hirano T (2007) Safety management based on detection of possible rock bursts by AE monitoring during tunnel excavation. Rock Mech Rock Eng 40:563–576

Inglada V (1928) Die Berechnung der Herdkoordinaten eines Nahbebens aus den Eintrittszeiten der in einigen benachbarten Stationen aufgezeichneten P- oder S-Wellen. Gerlands Beitr Geophys 19:73–98

Jiang F, Yang S, Cheng Y (2006) A study on microseismic monitoring of rock burst in coal mine. Chin J Geophys 49:1511–1516

Kijko A (1977a) An algorithm for the optimum distribution of a regional seismic network-I. Pure appl Geophys 115:999–1009

Kijko A (1977b) An algorithm for the optimum distribution of a regional seismic network-II: an analysis of the accuracy of location of local earthquakes depending on the number of seismic stations. Pure appl Geophys 115:1011–1021

Kijko A, Sciocatt M (1995) Optimal spatial distribution of seismic stations in mines. Int J Rock Mech Min Sci Geomech Abstr 32:607–615

Leighton F, Blake W (1970) Rock noise source location techniques. USBM RI 7432

Leighton F, Duvall WI (1972) A least squares method for improving rock noise source location techniques, USBM RI 7626

Li S (2009) Discussion on microseismic monitoring technology and its application to underground project. Chin J Undergr Space Eng 5:122–128

Luo X, Hatherly P (1998) Application of microseismic monitoring to characterize geomechanic conditions in longwall mining. Explor Geophys 29:489–493

Obert L (1975) The microseismic method: discovery and early history. Proc. 1st Conference of acoustic emission/microseismic activity in geological structures and materials. Clausthal-Zellerfeld: Trans. Tech. Publications pp 11–12

Obert L, Duvall I (1942) Use of sub audible noises for the prediction of rock bursts. Part II, RI 3654, USBM

Prugger A, Gendzwill D (1988) Microearthquake location: a non-linear approach that makes use of a Simplex stepping procedure. Bull Seismol Soc Am 78:799–815

Qian M, Shi P (2003) Mine pressure and strata control. China University of Mining and Technology Press, Xuzhou

Rindorf HJ (1981) Acoustic emission source location in theory and in practice. Bruel Kjaer Tech Rev 2:3–44

Rindorf HJ (1984) Location of microseismic activity: an algorithm for three-dimensional source location based on the arrival time differences among four pickup points, Proceedings Third Conference on acoustic emission/microseismic activity in geologic structures, Trans Tech Publications, Clausthal, Germany, pp 695–706

Sambridge M, Gallagher K (1993) Earthquake hypocenter location using genetic algorithms. Bull Seismol Soc Am 83:1467–1491

Shishay B, Heather D, Charlotte R (2012) Microseismic swarm activity in the New Madrid seismic zone. Bull Seismol Soc Am 102:1167–1178

Tang G (1979) A general method for determination of earthquake parameters by computer. Acta Seismol Sin 1:186–196

Thurber CH (1985) Nonlinear earthquake location: theory and examples. Bull Seismol Soc Am 75:779–790

Tian Y, Chen X (2002) Review of seismic location study. Prog Geophys 17:147–155

Xia Y, Lan H, Mao D, Pan J (2011) Study of the lead abutment pressure distribution base on microseismic monitoring. J China Univ Min Technol 40:868–873

Xu X, Sahni S, Rao NSV (2008) On basic properties of localization using distance-difference measurements, the 11th International Conference on Information Fusion, Cologne, Germany, pp 1–8

Xu N, Tang C, Li H (2011) Optimal design of micro-seismic monitoring array and seismic source location estimation for rock slope. Open Civil Eng J 5:36–45

Zhu Q, Jiang F, Wang C, Liu Y, Wang J, Yu Z (2013) Automated microseismic event arrival picking and multichannel recognition and location. J China Coal Soc 38:397–403